

# Simulations of the Weibel instability with a High-Order Discontinuous Galerkin Particle-In-Cell Solver

G. B. Jacobs, \* and J. S. Hesthaven†

*Division of Applied Mathematics, Brown University, 182 George Street, Providence, RI, 02912*

G. Lapenta

*Los Alamos National Laboratory, Los Alamos, New Mexico, 87545*

This paper presents a comparison of various particle-in-cell numerical methodologies for Weibel instability simulations. A convergence study with the established finite difference time domain particle-in-cell method establishes a base result. Comparison to novel particle-in-cell methods based on an implicit temporal discretization, and on a second and fifth order discontinuous Galerkin scheme (DG-PIC) provide insights into components of the DG-PIC schemes including divergence cleaning, particle weighing parameters and resolution requirements. High-order DG-PIC uses less grid points for a resolved solution making it competitive with the established finite difference method. Implicit time schemes nearly eliminate stability constraints.

## Nomenclature

$ CFL $	Courant-Friedrichs-Levy condition
$ E $	energy spectrum
$ \vec{E} $	electric field vector
$ \vec{H} $	magnetic field vector
$ \vec{k} $	wave vector
$ m $	particle mass
$ N $	number of grid edges along a boundary
$ N_p $	initial number of particles in one direction
$ p $	polynomial order of triangle polynomial
$ q $	particle charge
$ r $	radial coordinate of particle deposition function
$ S(r) $	particle deposition function
$ t $	time
$ u $	velocity in $x$ -direction
$ v $	velocity in $y$ -direction
$ \alpha $	power on distribution function
$ \Delta x $	grid spacing
$ \Delta t $	time step
$ \lambda_{De} $	Debye length
$ \omega_{pe} t $	plasma frequency
$ \rho $	charge density
$ \chi $	multiples of light speed at which divergence is cleared
<i>Subscript</i>	

---

\*Visiting Assistant Professor, AIAA member.

†Professor

*e* electron  
*th* thermal  
*p* particle

## I. Introduction

The reliable, accurate, and efficient computational modeling of plasma dynamics remains very challenging. Plasma dynamics span from the smallest (atomistic particle-particle dynamics) to the largest scales like solar flares and galaxy dynamics. Plasmas also exhibit a strong interaction between the many scales and the long range electromagnetic forces. Moreover, the range of applications is very broad, e.g., fusion energy, both by means of magnetic confinement and laser ignited devices; high-power microwave generation; large scale particle accelerators; and a variety of plasma based technology. This warrants that significant resources be spent on the development of accurate, robust, and efficient tools for the modeling of such plasma problems.

Particle-in-cell (PIC) methods have proved a valuable tool for the modeling of a variety of plasma problems. In this approach typically the electric and magnetic field are solved by means of the Maxwell equations and/or a Poisson equation in the Eulerian framework. Charged plasma particles are forced by the fields and tracked in a Lagrangian framework. Particles are coupled with the field solver by weighing the sum of the Coulomb forces onto the grid in the form of a charge or current density.

A number of methods based on this idea has been developed. The exact charge conserving scheme proposed in Ref. 1 is widely used since it eliminates the need to directly impose Gauss law to ensure charge conservation. In Ref. 2 this technique is extended to include a multi-block body-fitted finite element method with the aim of increasing geometric flexibility. Umeda et al.<sup>3</sup> suggest a zigzag particle trajectory to improve upon the computational efficiency in Ref. 1, while in Ref. 4 the time step restriction of explicit methods is tackled with an implicit Maxwell solver. All of these methods are second order accurate in space and time and are, in most cases, restricted to simple Cartesian or block structured geometries.

In Jacobs and Hesthaven,<sup>5</sup> a PIC algorithm based on a high-order nodal discontinuous Galerkin solver (DG-PIC) was introduced. The DG Maxwell's solver<sup>6</sup> has low dispersion, geometric flexibility and excellent stability properties. These properties have made DG superior for long time integration problems, complex geometries, and high frequency electromagnetics problems. DG-PIC has in principle the same potential for plasma simulations making it a viable alternative for the simulation of dense, high frequency, high power relativistic plasmas found in for example high-power microwave devices and laser-matter interaction problems.

The DG-PIC algorithm uses smooth, flexible and computationally efficient particle distribution functions that reduce the finite grid instability troubling traditional finite-difference time-domain PIC were introduced. A spectral levelset solver allows for the treatment of complex geometrical particle boundary conditions. A fully explicit, hyperbolic Lagrangian multiplier method is shown to be accurate and robust for divergence cleaning. High-order Runge-Kutta schemes ensure high-order temporal accuracy that has previously only been second order.

This paper presents benchmark plasma simulations<sup>7</sup> of the Weibel instability using the explicit high-order nodal Discontinuous Galerkin particle-in-cell (DG-PIC) method.<sup>5</sup> The properties of the scheme are studied by comparing to several other established numerical methodologies including an explicit<sup>9</sup> and implicit finite difference solver<sup>8</sup> on structured and unstructured grids.<sup>10</sup> It is shown that the high-order method requires fewer grid points per wave number to resolve a plasma flow, and has favorable stability properties.

In the remainder of the paper we first give a brief overview of the numerical methodologies and their properties. Then we show results of the Weibel instability. The final section is reserved for conclusions.

## II. Brief Overview of Numerical Methodologies

The algorithms considered in this paper are all of the particle-in-cell (PIC) type. All PIC algorithms consist of a Maxwell field solver, a particle tracker and a particle assignment. We compare the classic explicit finite difference time domain (EFDTD) method,<sup>9</sup> the implicit finite difference time domain method (IFDTD),<sup>4</sup> and the DG-PIC method.<sup>5</sup>

## A. Spatial Discretization

The spatial discretization for explicit and implicit FDTD PIC solvers are both based on a second-order finite difference discretization to solve the Maxwell's equations. The particle assignment employs area weighing within a cell and is second order. Second order interpolation is used for interpolation of the field variables to the particle position. The DG-PIC method discretizes the Maxwell's equations differently through a high-order discontinuous Galerkin method. The particle assignment directly projects a smooth particle shape function onto the grid, that may span more than one cell. High-order interpolation of the same order as the approximation order in an element determines the field variables at the particle location. A second-order DG-PIC that weigh particles linearly within each triangle<sup>10</sup> of the unstructured is also considered in this paper.

## B. Temporal discretization

EFDTD uses the well-known second-order leap-frog scheme for both the Maxwell's and particle update. IFDTD uses a second-order implicit time integration of both the field and particle equations. DG-PIC updates the field and particles with an explicit Runge-Kutta scheme generally of fourth order. Alternatively DG-PIC uses an additive fourth order Runge-Kutta scheme<sup>11</sup> which is implicit for the field solver and explicit for the particle tracker.

## C. Divergence cleaning

Electromagnetic field solvers usually satisfy the Gauss laws in time if they are initially satisfied. Most PIC solvers, however, require an explicit solution of the electric Gauss law as a result of the charge density source in the Gauss law. To this end, the FDTD solvers use Boris projection method.<sup>9</sup> The DG-PIC method uses the Boris method as well. Since Boris method reduces the scheme's order of approximation, a hyperbolic Lagrangian Multiplier Method<sup>12</sup> is also considered. The hyperbolic cleaning method clears divergence away at  $\chi$ -multiple characteristic velocities of the light speed and then dissipates it. Increasing  $\chi$  improves the physical representation of the model. This method does not suffer from reduced accuracy, but it increases the stiffness of the modified Maxwell's equation, making it more computationally expensive. This is a restriction that is relaxed through an implicit field solver.

# III. Some theoretical implications

## A. Stability

Instability generally manifests itself in the form of a total energy increase, also called grid heating. The explicit PIC approach is subject to three stability constraints, i.e. to prevent grid heating EFDTD requires  $\Delta t < \Delta x/c$ ,  $\Delta t < 2/\omega_{pe}$ , and  $\Delta x/\lambda_{De} < \zeta$ , Here,  $\omega_{pe}$  is the electron plasma frequency,  $\lambda_{De}$  is the Debye length and  $\zeta$  is a constant. The first condition is the Courant condition, the second introduces a constraint related to the fastest electron response time and the final constraint relates to an aliasing instability resulting from interpolation between grid and particles. IFDTD does not suffer from the first two stability constraints,<sup>13</sup> but an accuracy condition may be formulated as  $v_{th}\Delta t < \Delta x$ , whose principal effect is to determine how well energy is conserved. IFDTD is also less affected by aliasing.<sup>13</sup> DG-PIC is restricted by all three stability constraints. However, DG requires less resolution than FDTD resulting in larger grid spacings and thus larger allowable time steps. Moreover, aliasing errors are smaller for smooth particles on a high-order grid.

## B. Dispersion

The EFDTD leap frog scheme requires that the cfl criterion,  $cfl = \Delta t\sqrt{2}/\Delta x < 1.0$ . For a cfl criterion less than 1 the scheme is dispersive and generally cfl is chosen very close to 1. The dispersion relation in IFDTD is adjustable.<sup>13</sup> High-order DG methods have virtually no dispersion.

### C. Cherenkov radiation

The inherent dispersion properties of the finite-difference approximation result in an artificial numerical Cherenkov radiation when modeling highly relativistic problems.<sup>14</sup> This purely numerical pollution of the solution is the result of the concave nature of the field solver's numerical dispersion relation, causing fast waves to propagate slower than is physically correct. In highly relativistic problems the unphysical interaction of fast particles with these waves create a Cherenkov radiation. DG has a strictly convex dispersion relation and does not suffer from Cherenkov radiation.

### D. Accuracy

FDTD methods require 30-50 points per wavenumber. For the DG-PIC method at fourth/fifth order 10-12 points per wavenumber suffice.

## IV. Weibel Instability

This section revisits the PIC simulations of the Weibel instability presented in Morse and Nielson,<sup>7</sup> who used a FDTD method. Here, a convergence study with FDTD is conducted first. The converged results is used as a base for comparison to DG-PIC.

### A. Model

The Weibel instability simulations are performed on a unit square with periodic boundary conditions. A quasi-neutral with stationary ions and with an electron thermal velocity ratio of 5 of the velocity in  $x$ ,  $u_{th} = 0.25$  and  $y$ ,  $v_{th} = 0.05$  direction, initiates the simulation. The plasma frequency is fifteen times the length of the square, i.e.  $\omega_{pe} = 15$  resulting in  $\frac{q}{m} = -(\pi 15)^2$  with the electron charge density set to  $\rho = -1$ .

From these initial conditions, magnetic waves develop with a dominant frequency in  $y$ -direction. The wave number decreases in time as the thermal velocities go to the equilibrium state. Throughout this section, a time interval of  $t=2$  is considered.

### B. Explicit finite difference time domain: EFDTD

This section presents a convergence study is conducted for EFDTD using grids with  $N=32, 64, 128$ , and  $256$ . 36 cells per particles are inserted for all  $N$ .

#### 1. Energies

Figure 1 compares various plasma energy components. With increased resolution the total energy conservation improves. The percentage total energy increase over a simulation time of  $t=2$  is 170%, 11%, 3%, and 0.6% for  $N=32, 64, 128$ , and  $256$ , respectively.

To avoid the total energy increase, indicative of grid heating, the Debye length needs to be resolved. The Debye length  $\lambda_{De}$  based on the smallest thermal velocity in  $y$ -direction is  $\frac{v_{th}}{\omega_{pe}} = 0.05/15 = 0.0033$ . At  $N = 256$  the smallest grid spacing is  $h = 0.0039$ , thus nearly resolving the Debye length.

The kinetic energy is known to closely follow the total energy increase caused by grid heating. Figure 1 confirms this finding. Only for  $N=128$  and  $256$  do we recognize the true trend of the kinetic energy, i.e. it first decreases slightly after which it levels off. Kinetic energy is exchanged for magnetic energy, i.e. the magnetic energy first increases after which it slowly decreases in the time interval considered. The electric energy seems unchanged in time. For higher resolution the fluctuation in it decreases; the improved resolution reduces noise in the charge density, which carries over to the electric field through the Poisson equation.

#### 2. Energy spectra

Figure 2 compares the  $H_z$  and  $E_x$  energy spectra for  $N=64, 128$  and  $256$  at  $t=2.0$ . The spectra,  $E(|\vec{k}|)$ , are determined by integrating the Fourier transforms of  $H_z$  and  $E_x$  over a circular surface in the  $\vec{k}$  wave space, effectively eliminating directional information of the Fourier transform. The energy spectrum gives an indication of the energy distribution over the wavenumbers. The  $H_z$  spectrum shows that most of the

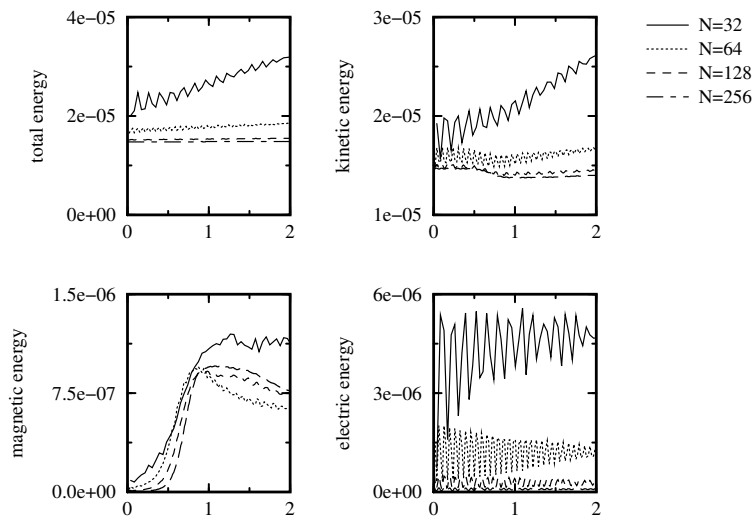


Figure 1. Various plasma energy components for EFDTD simulations at resolutions  $N=32$ ,  $64$ ,  $128$ , and  $256$ .

energy is stored in the region  $0 < |k| < 7$ . For  $N=128$  and  $256$  the  $H_z$  spectra are nearly identical in the range  $|\vec{k}| < 10$ .  $N=256$  shows a better drop-off for  $|\vec{k}| > 10$  than  $N=64$  and  $128$ , a result of improved resolution. The inability of the finite difference method to capture high wavenumbers effectively leads to an energy increase for larger  $|\vec{k}|$ . The wavenumber at which the spectrum increases provides an indication of the maximum wave number that is accurately resolved. This yields  $|\vec{k}_{max}| \sim 10, 20$  and  $40$  for  $N=64, 128$ , and  $256$ , respectively. The  $E_x$  energy spectra shows no dependency on  $|\vec{k}|$ , an indication of the dominance of noise in the electric field. Increasing  $N$  reduces this noise, leading to the decreased energy spectrum.

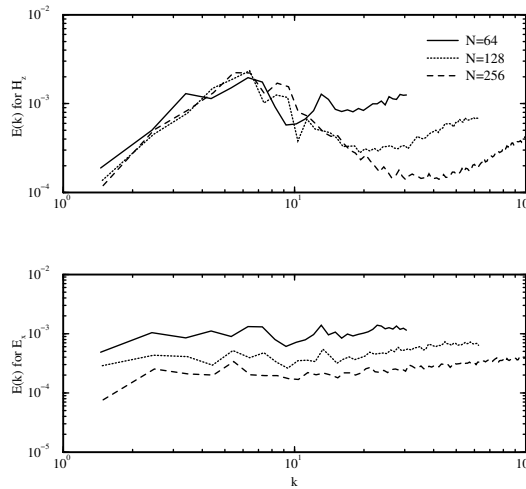
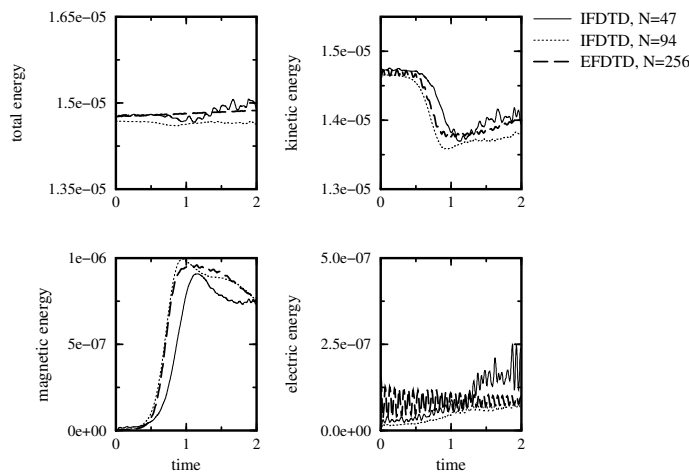


Figure 2. Comparison of  $H_z$  and  $E_x$  energy spectra for  $N=64, 128$ , and  $256$  at  $t=2$  using an EFDTD method.

### C. Implicit finite difference time domain: IFDTD

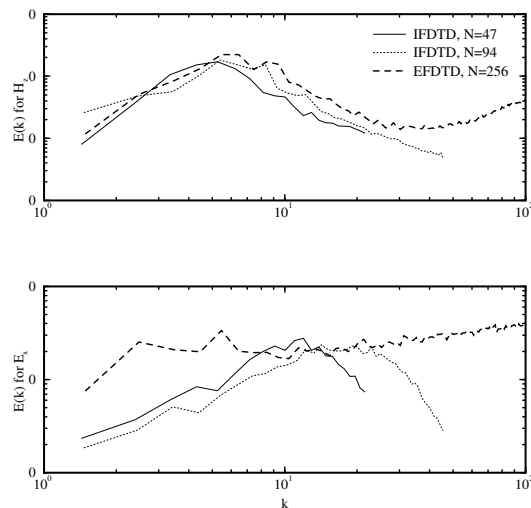
This section presents results of simulations using an implicit second-order finite difference method.<sup>13</sup> The simulations are performed on a  $47 \times 47$  and a  $94 \times 94$  grid. Both simulations are initialized with 64 particles per cell.



**Figure 3.** Comparison of various plasma energy components for a 2nd order implicit finite difference with resolution  $N=47$ , and  $94$ .

Figure 3 compares the various plasma energy components for the two cases to the EFDTD result. The total energy conservation improves with resolution. At  $N=94$  the conservation is comparable to the EFDTD result with resolution  $N=256$ , i.e IFDTD is less affected by the finite grid instability.<sup>13</sup> The kinetic energy and magnetic energy has converged to the EFDTD result at  $N=94$ . The electric energy noise reduction with increased  $N$  confirms that the electric field is mostly influenced by noise in the charge density.

## 2. Energy spectra



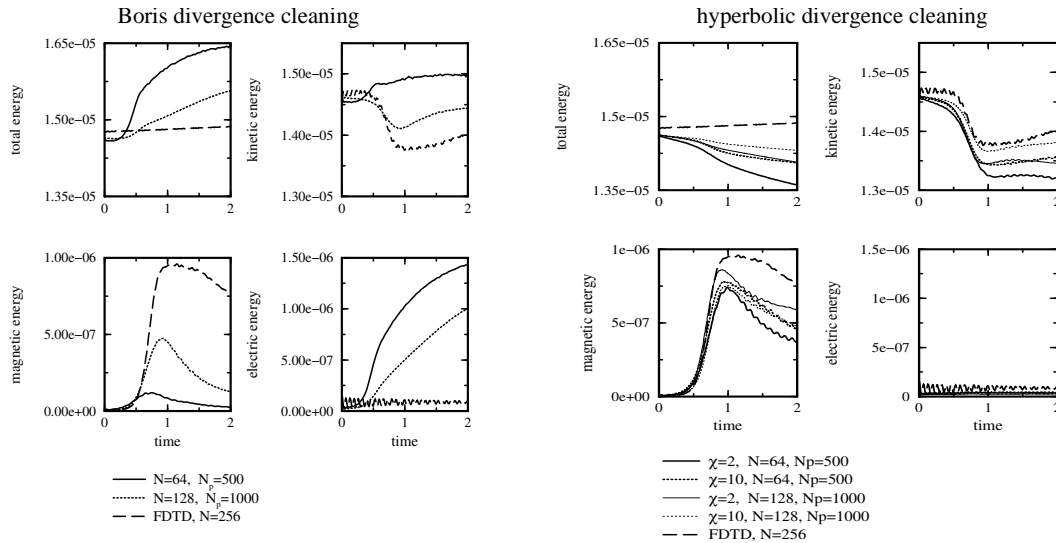
**Figure 4.** Comparison of  $H_z$  and  $E_x$  energy spectra for IFDTD with  $N=47$ , and  $94$  to EFDTD with  $N=256$  at  $t=2$ .

Figure 4 compares the energy spectra between IFDTD and EFDTD. IFDTD does not display the EFDTD's increase in the spectra at large  $|\vec{k}|$ . We conclude that IFDTD has a dissipative nature, possibly related to the implicit time scheme. The IFDTD  $H_z$  spectra converge to the EFDTD result.

## D. Second order DG-PIC

This section presents results of simulations using a second order DG-PIC method. In this approach particles are weighed to the grid with a linear area weighing technique per triangle,<sup>10</sup> rather than the smooth large particle used for the higher order DG-PIC. Simulations are performed on 64x64x2 equidistant grid with 500x500 particles and on a 128x128x2 equidistant grid with 1000x1000 particles, identified with  $N=64$  and  $N=128$ , respectively. Both Boris and hyperbolic divergence cleaning are considered.

### 1. Energies



**Figure 5. Comparison of various plasma energy components for 2nd order simulations with Boris and hyperbolic divergence cleaning.**

Figure 5 compares

the evolution of various plasma energy components in time for simulations with a Boris and a hyperbolic divergence cleaning with  $\chi=2$ , and 10.

The Boris divergence cleaning cases show  $\sim 14\%$  and  $6\%$  total energy increase at  $t=2$  for  $N=64$  and 128, which compares to the  $N=64$  and 128 EFDTD energy increase. The solution using hyperbolic divergence cleaning exhibits a decreased total energy. This energy dissipation is caused by the divergence damping. Increasing  $\chi$  and  $N$  reduces grid heating. At  $\chi=10$  and  $N=128$  the total energy deviation is  $2\%$ .

The kinetic energy closely follows the total energy for the Boris method cleaning as is the case for the EFDTD method. The kinetic energy for the hyperbolic cleaning is similar to the converged the EFDTD solution.

The reduced accuracy of the Boris solution, making the global method first order, is particularly noticeable through the significantly smaller peak in the magnetic energy trend. The hyperbolic cleaning method shows better comparison in the peak value, but still underestimates it. Interesting is the similar solution for  $\chi=10$  at  $N=64$  and 128. This suggests that the solution is nearly converged. Note that the Debye length is approximately resolved at  $N=128$ . Thus convergence is expected.

The electric energy trend for the Boris method expectedly shows the same dependency on  $N$  as the EFDTD method that uses the Boris cleaning too. The fluctuation in the electric energy for the hyperbolic cleaning method is one order less than EFDTD, a result of the damping.

### 2. Energy spectra

The energy spectra (Fig. 6) confirm the general conclusion made above, i.e. the resolved hyperbolic cleaning method is in decent agreement with the resolved EFDTD result, whereas the Boris solution is underresolved. We also observe that DG-PIC does not display an increase in the  $H_z$  spectrum at large  $|\vec{k}|$ . The upwind nature

of the DG scheme results in damping of the high-frequency waves, leading to a drop-off in the spectrum. The central EFDTD scheme does not dissipate these waves.

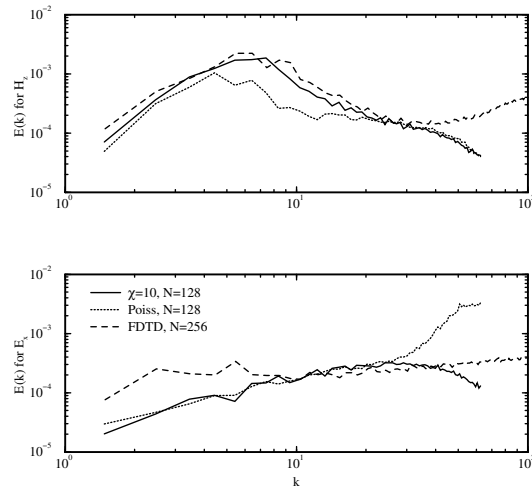


**Figure 6.** Comparison of  $H_z$  and  $E_x$  energy spectra for EFDTD and a second order DG-PIC method using Boris and hyperbolic cleaning at  $t=2$ .

### E. Fifth order Discontinuous Galerkin: DG-PIC

This section presents results of simulations using a fifth order DG-PIC method. There are a number of parameters in this method that determine resolution. The following notation identifies these parameters:

- $N$  identifies the number of edges along the side of the square yielding  $N \times N \times 2$  triangular elements in the computational domain. Most computations use  $N=10$ .
- $p$  the polynomial order of each element. All simulations presented in this section use  $p=4$ , i.e. fifth order scheme.
- $N_p$  the number of particles (initially equidistantly placed) in one direction yielding  $N_p \times N_p$  particles in the domain.
- $R$  the radius of the isotropic particle distribution function.
- $\alpha$  the power of the distribution function,  $S(r) = \frac{\alpha+1}{\pi R^2} \left[1 - \left(\frac{r}{R}\right)^2\right]^\alpha \quad r = 0 \dots R..$

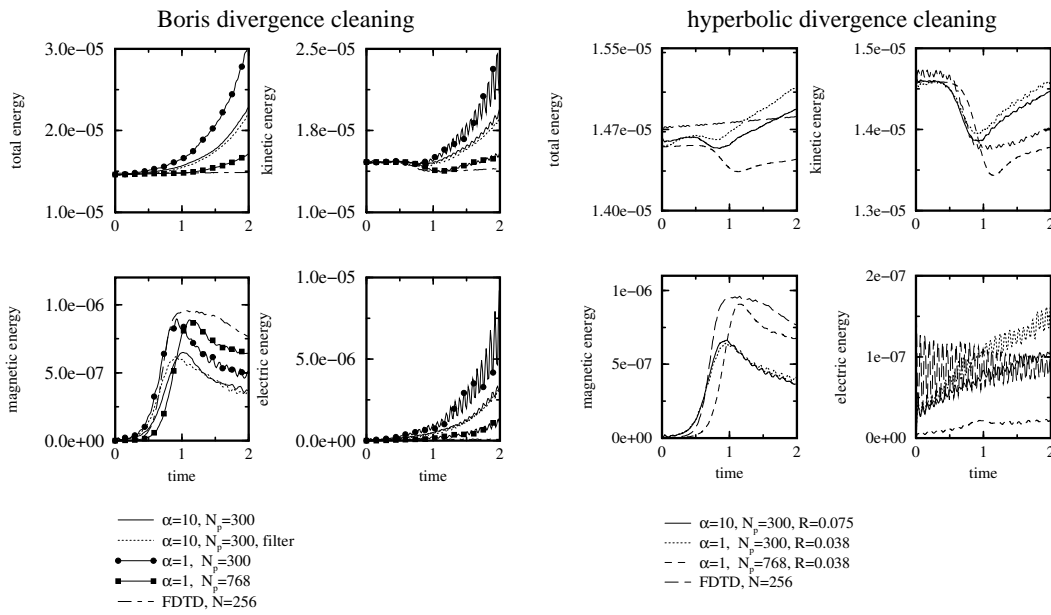
#### 1. Energies

Figure 7 compares the evolution of various plasma energy components in time. Again, it is observed that the hyperbolic cleaning method conserves energy better with less than 3% deviation as compared to 10-50% increase with Boris cleaning for similar resolutions. Unlike the second order method, the fifth order method exhibits total energy increases for the hyperbolic cleaning method. This is possibly related to the larger particles enhancing grid heating and/or the increased numerical dissipation of the second order method compared to the fifth order method.

The fifth order methods show comparable trends for the kinetic energy, i.e. first decrease followed by a slow increase. With more particles the Boris method method improves on capturing the particle kinetics.

The magnetic energy trend is captured by both methods. The fifth order methods predicts a smaller peak value compared to the EFDTD as is the case for the second order unstructured method. Increasing the number of particles increases the peak value.

Hyperbolic cleaning is superior in reducing noise in the electric energy. The fifth order Poisson method shows noise levels comparable to the  $N=64$  EFDTD method.



**Figure 7. Comparison of various plasma energy components for fifth order DG-PIC simulations of the Weibel instability with Boris and hyperbolic divergence cleaning.**

Surprisingly, it is observed that decreasing  $\alpha$  has a minimal effect on the energy trends. Note that for  $\alpha=1$   $R$  is taken half the value as compared to  $\alpha=10$ . The reason is that at  $\alpha=10$  most of the deposition function is located within the half radius near the origin. For  $\alpha=1$  the deposition in this region is approximated with a linear function. The simplified function and reduced influence region lead to a factor three speed up.

Decreasing  $\alpha$  with Boris cleaning leads to poorer energy conservation as one would expect (larger aliasing error) resulting in worsened energy trends. This is not the case for the hyperbolic cleaning. It is not clear why this difference is so obvious. Applying a weak filtering on the Poisson source term reduces grid heating, however it doesn't necessarily improve the results as witnessed in the magnetic energy trend.

## 2. Energy spectra.

The energy spectra in Fig. 8 show that the high-order simulations show a drop in the spectrum caused by the diffusion of the upwind numerical flux. The  $H_z$  spectra are not affected much by  $\alpha$  and a moderate filter. Increasing the number of particles increases the drop off at high wave numbers. Decreasing  $\alpha$  and decreasing  $N_p$  introduces more energy in the low wavenumber part of the  $E_x$  spectrum. The filter has little effect on the  $E_x$  spectrum as well. The  $E_x$  spectrum of the high order method with hyperbolic divergence cleaning compares better to the EFDTD result than the results obtained with the Boris divergence cleaner.

## F. Thermal velocity

The thermal  $u$  and  $v$  velocity at time  $t=2$ , tabulated in Table 1 for the methods discussed above. It shows that all methods considered converge to one result. From this table one concludes that the results for  $\chi=10$  compare best with the EFDTD result. Increasing  $\chi$  from 2 to 10 has quite an effect on the velocities indicating that the less physical  $\chi=2$  simulations should not be considered.

## G. Time step

The time step for all methods in this paper is bound by stability constraints. The grids for at which the simulations are converged yield a time step of  $\Delta t=2.7e-3$ ,  $2.1e-3$ ,  $1.4e-3$ , and  $9e-3$ , EFDTD, IFDTD, second order DG-PIC, and fifth order DG-PIC. The high-order DG-PIC method allows for a significantly larger time step than the low order explicit methods. This speeds up computations. We did not investigate convergence

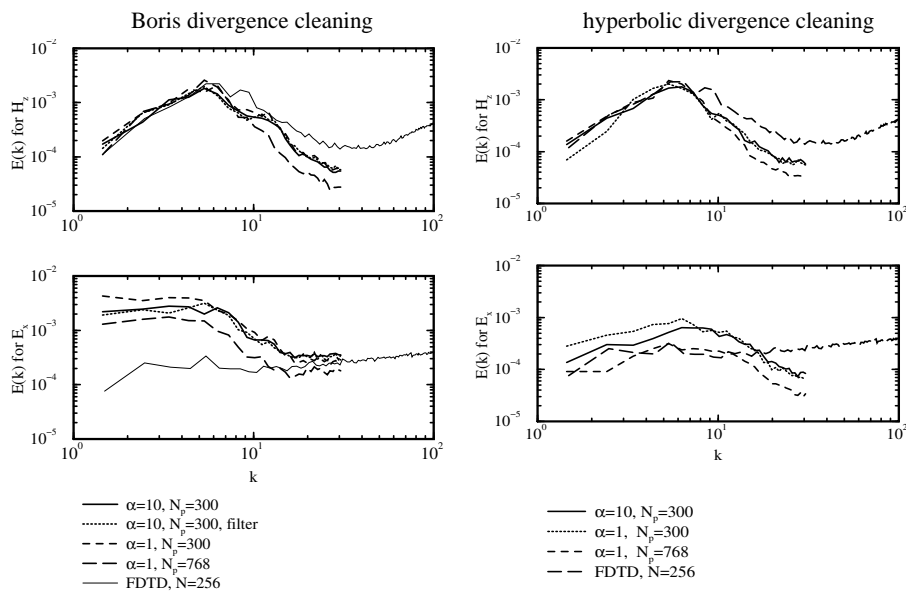


Figure 8. Comparison of  $H_z$  and  $E_x$  energy spectra for fifth order DG-PIC simulations of the Weibel instability with Boris and hyperbolic divergence cleaning at  $t=2$ .

of IFDTD with time step, but we anticipate that IFDTD will be accurate at time steps comparable to the DG-PIC simulation.

## V. Conclusion

Simulations of the Weibel instability have clarified a number of characteristics of a particle-in-cell method based on a discontinuous Galerkin method (DG-PIC).

Most importantly, high-order DG-PIC use less points and a larger time step to resolve the Weibel instability as compared to second order methods. This will save memory and computational for larger computations. Moreover, DG-PIC dissipates high-frequency waves as a result of its upwind character as opposed to a central finite difference molecule for which high frequency wave have the potential to pollute the solution. A hyperbolic divergence cleaner is more accurate and appears more robust than a Boris projection based divergence cleaner. The hyperbolic cleaner requires clearance of divergence with velocities of at least ten times the speed of light. For isotropic simulations a smooth particle distribution does not decrease grid heating significantly compared to a linear particle distribution.

Implicit particle-in-cell methods nearly eliminate stability issues, allowing for lower resolutions without accuracy penalties. Combining the implicit methodology with DG-PIC is thus promising. We hope to present this type of algorithm in future work.

## Acknowledgments

The authors thank Dick Morse from Los Alamos National Laboratory for suggesting the Weibel instability simulation for testing.

## References

- <sup>1</sup>Villasenor, J. and Buneman, O., "Rigorous charge conservation for local electromagnetic field solvers," *Comput. Phys. Comm.*, Vol. 69, 1992, pp. 306–316.
- <sup>2</sup>Eastwood, J. W., Arter, W., Brealey, N. J., and Hockney, R. W., "Body-fitted electromagnetic PIC software for use on parallel computers," *Comput. Phys. Comm.*, Vol. 87, 1995, pp. 155–178.
- <sup>3</sup>Umeda, T., Omura, Y., Tominaga, T., and Matsumoto, H., "A new charge conservation method in electromagnetic particle-in-cell simulations," *Comput. Phys. Comm.*, Vol. 156, 2003, pp. 73–85.

Scheme	$\alpha$	$R$	$N_p$	$u_{the}$	$v_{the}$	$u_{the} - v_{the}$
IFDTD ( $N=47$ )				0.202	0.137	0.065
IFDTD ( $N=94$ )				0.205	0.142	0.063
Poisson (2nd, $N=64$ )				0.193	0.1714	0.0216
Poisson (2nd, $N=128$ )				0.202	0.151	0.051
$\chi=10$ (2nd, $N=64$ )				0.200	0.142	0.058
$\chi=10$ (2nd, $N=128$ )				0.204	0.140	0.063
$\chi=2$	10	0.075	300	0.198	0.151	0.047
$\chi=2$	1	0.038	300	0.202	0.148	0.054
$\chi=2$	1	0.038	768	0.204	0.137	0.067
$\chi=10$	10	0.075	300	0.208	0.145	0.062
$\chi=10$	1	0.038	300	0.207	0.147	0.060
$\chi=10$	1	0.038	768	0.205	0.138	0.067
Poisson	10	0.075	300	0.227	0.187	0.040
Poisson	1	0.038	300	0.237	0.194	0.043
Poisson	1	0.038	768	0.212	0.154	0.058
EFDTD ( $N=64$ )				0.219	0.161	0.058
EFDTD ( $N=128$ )				0.207	0.146	0.061
EFDTD ( $N=256$ )				0.206	0.140	0.066

**Table 1. Comparison of thermal velocities for second and fifth order DG-PIC and EFDTD PIC at  $t=2$ .**

<sup>4</sup>Vu, H. X. and Brackbill, J. U., "CELESTE1D: An implicit, fully kinetic model for low-frequency, electromagnetic plasma simulation," *Comput. Phys. Comm.*, Vol. 69, 1992, p. 253.

<sup>5</sup>Jacobs, G. B. and Hesthaven, J. S., "High-order nodal discontinuous Galerkin particle-in-cell method on unstructured grids," *J. Comp. Phys.*, 2005. to appear.

<sup>6</sup>Hesthaven, J. and Warburton, T., "Nodal high-order methods on unstructured grids. I. Time-domain solution of Maxwell's equations," *J. Comp. Phys.*, Vol. 181, 2002, pp. 186–221.

<sup>7</sup>Morse, R. L. and Nielson, C. W., "Numerical Simulation of the Weibel Instability in One and Two Dimensions," *Phys. Fluids*, Vol. 14, No. 4, 1971, pp. 830–840.

<sup>8</sup>Ricci, P., Brackbill, J. U., Daughton, W., and Lapenta, G., "Collisionless Magnetic Reconnection in the Presence of Guide Field," *Phys. Plasmas*, Vol. 11, No. 8, 2004, pp. 4102–4144.

<sup>9</sup>Birdsall, C. K. and Langdon, A. B., *Plasma physics via computer simulation*. McGraw-Hill, Inc., 1985.

<sup>10</sup>Seidel, D., Pasik, F., Kiefer, M., Riley, D., and Turner, C., "Advanced 3D electromagnetic and particle-in-cell on structured/unstructured hybrid grids," SAND97-3190, Sandia National Laboratory, Livermore, CA, 1998.

<sup>11</sup>Kennedy, C. and Carpenter, M., "Additive Runge-Kutta schemes for convection-diffusion-reaction equations," *Appl. Num. Math.*, Vol. 44, 2003, pp. 129–181.

<sup>12</sup>Munz, C. D., Omnes, P., Schneider, R., Sonnendruker, E., and Voss, U., "Divergence correction techniques for Maxwell solvers based on a hyperbolic model," *J. Comp. Phys.*, Vol. 161, 2000, pp. 484–511.

<sup>13</sup>Lapenta, G. and Brackbill, J. U. and Ricci, P., "Kinetic Approach to microscopic-macroscopic coupling in space and laboratory plasmas", submitted, 2006.

<sup>14</sup>Greenwood, A., Cartwright, K., Luginsland, J., and Baca, E., "On the elimination of numerical Cherenkov radiation in PIC simulations," *J. Comp. Phys.*, Vol. 201, 2004, pp. 665–684.